Reaction Rate of $Ti_{0.18}Zr_{0.84}Cr_{1.0}Fe_{0.7}Mn_{0.3}Cu_{0.057}$ to Use for the Heat Driven Type Compact Metal Hydride Refrigerator*

Sang-chul BAE† and Masafumi KATSUTA‡

Abstract

Our final goal of this study is to develop the heat driven type compact metal hydride (MH) refrigeration system for the vending machine and the show case, and to attain a refrigeration temperature of 243 K by using a heat source of about 423K. The reaction rate of the MH to use for the heat source, MH used for heat source is studied firstly because the MH refrigeration system consists of two MHs, one is used for the heat source and the other is used for the cooling load extracting. As for the reaction rate in the hydriding process, initially, a rapid surface reaction, governed by the relation $1-(1-F)^{1/3}=k_h t$. After the MH surface has been covered by hydride, the reaction becomes diffusion controlled with the relation $1-3(1-F')^{2/3}+2(1-F')=k_h' t$. The reaction rates, k_h and k'_h, are exponentially proportional to the pressure difference and increase with temperature. And, as for the dehydriding process, it is found out that the rate-controlling step is uniquely diffusion reaction. The dehydriding reaction rate is exponentially proportional to the pressure difference and the initial reacted fraction, and increases with temperature. Finally, on the basis of these experimental results, the brand new rate correlations are reasonably derived. The predicted results for this correlation are in successfully agreement with the experimental ones.

Key Words : *Reaction rate, Plateau pressure, Rate-controlling step, Reacted fraction*

Nomenclature

A	: Surface area (m^2)
C	: Heat capacity (J/K)
c	: Hydrogen concentration (wt %)
Di	: Diffusion reaction coefficient (cm^2/s)
E	: Activation energy ($J/molH_2$)
F	: Reacted fraction ($c/c_{max.}$)
dF/dt	: Reaction rate
k	: Reaction rate constant
ks	: Surface reaction rate constant (cm/s)
P	: Pressure (MPa)
R	: Gas constant (J/kgK)
r	: Radius (mm)
x	: Mass(g)
T	: Temperature (T)
t	: Time (s)

Greek letters

ΔH	: Reaction enthalpy ($J/molH_2$)
ΔP	: Pressure difference (MPa)
λ	: Effective thermal conductivity (W/mK)
δ	: Thickness (mm)
ρ	: Packing density (kg/m^3)

Subscripts

di	: Diffusion reaction
d	: Dehydriding reaction
h	: Hydriding reaction
high	: Used at a higher temperature for heat source
nc	: Temperature constant
p	: Plateau
s	: Surface
v	: Volume
l	: Initial
max.	: Maximum

1. Introduction

Recently, the cascade use of the energy, especially low-quality thermal energy, is desired all over the world, to achieve the reduction of CO_2 discharge amount regulated by COP3 Kyoto Protocol and to conserve the energy source. In the refrigeration field, the research on a refrigerator using waste heat and natural energy attracts attention from such demand. One of the promising candidates is Metal Hydride (MH) refrigeration system [1, 2].

In order to design the heat exchanger to use for the heat driven type MH refrigerator, we must satisfy the next heat flow equation [3].

* Received : September 26, 2005, Editor: Akira YABE

† Institute of Ocean Energy, Saga University (1 Honjo-machi, Saga, Saga, 840-8502, JAPAN)

‡ Department of Mechanical Engineering, Waseda University (3-4-1 Okubo, Sinjuku-ku, Tokyo, 169-8555, JAPAN)

$$\frac{\Delta H \cdot c_{max.} \cdot x}{2.016 \cdot 100} \frac{dF}{dt} = \frac{\lambda A}{\delta}(T - T_s) + C\frac{dT}{dt} \qquad (1)$$

where $c_{max.}$ is the hydrogen concentration (metal hydride) of equilibrium pressure 1.5 MPa at every temperature,$\lambda A/\delta$ is the heat transfer factor (λ, A and δ are the MH effective thermal conductivity, area and thickness respectively), C is the heat capacity of a system and dF/dt is the reaction rate.

In this paper, our interests firstly focused to the determination of the reaction rate, namely, dF/dt in the heat flow equation [3]. Then, the dF/dt of MH_{High} (MH used at a higher temperature for heat source) is studied.

2. Experimental apparatus and methods

2.1 Experimental apparatus

Figure 1 shows details of the experimental apparatus. The pipeline of this apparatus is mainly composed of stainless steel, 6.35mm O.D. (1/4 in) tube. Three points of temperature, environment air, at temperature constant bath and reservoir are measured by using mineral insulated thermo-couple (T type) of 1mm O.D. in the experiment. The two points of pressure in reservoir and reactor are measured with a strain gauge. The vacuum level in the system is measured with the vacuum gauge. The accuracy of the temperature and pressure measurement were ± 0.1 ℃ and ± 25 Pa, respectively. The sampling interval of measurements is about 0.17 s in case of integration time 16.7 msec. MH alloy is crushed beforehand and the average initial diameter of MH using our experiment is about 0.43 mm. In this research, the capacity method (Sievert's method) is used as a method of measuring the hydrogen storage capacity and reaction rate of MH alloy. In the Sievert's method, the hydrogen storage capacity of MH alloys is calculated from the pressure change before and after the equivalence state of two containers of already-known capacity, reservoir and reactor. Therefore, the precise capacity measurement of reservoir and reactor are important. The accuracy of capacity measurement is $\pm 0.1\ cm^3$.

PCT (Pressure-Concentration-Temperature) curve measurement based on the vacuum condition was used as an origin point of the hydrogen storage capacity of the MH alloy. Moreover, details of these methods are based on Japan Industrial Standards (JIS).

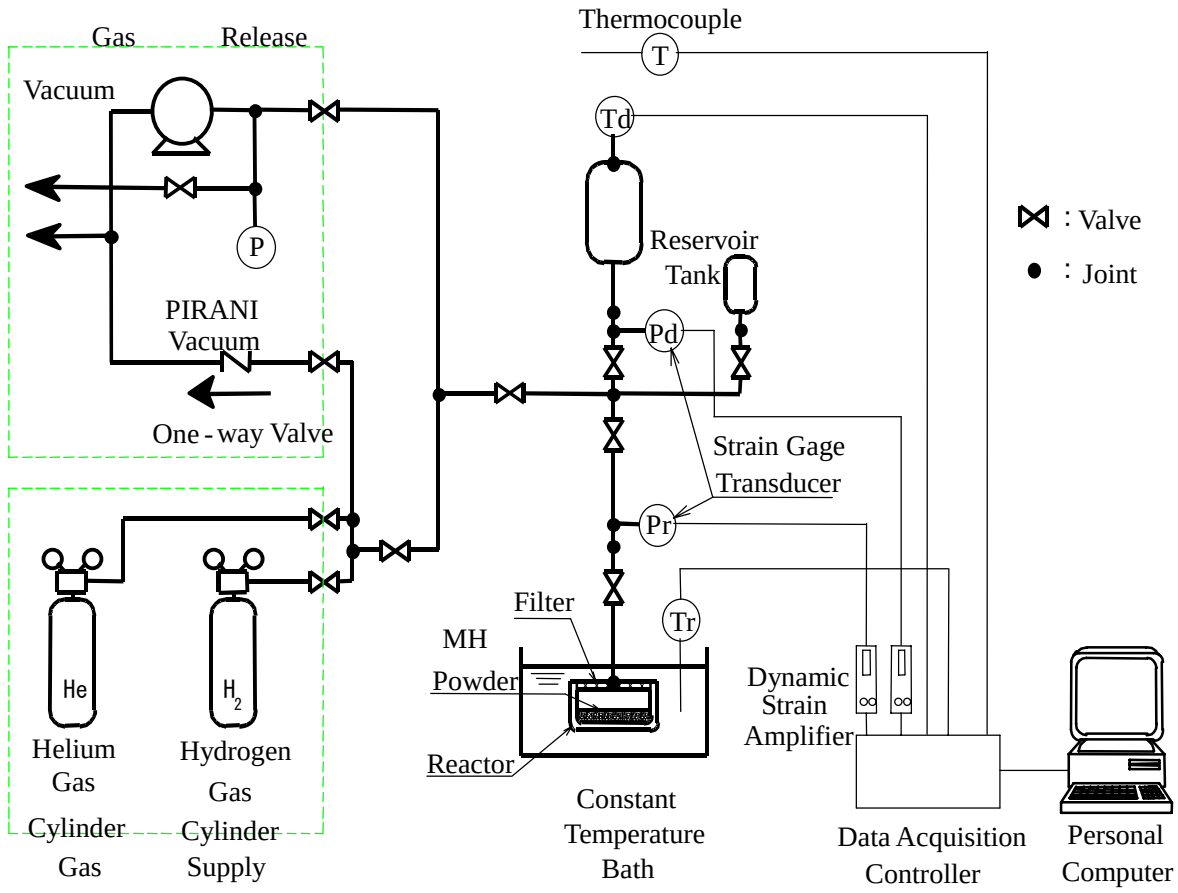

Fig. 1 Schematic Diagram of Experimental Facility

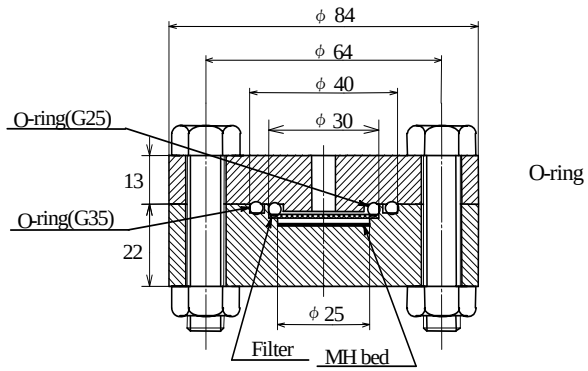

Fig. 2 Detail of Reaction Rate Measuring Reactor

2.1.1 Reactor for Reaction rate measurement

MH reactor was made of stainless steel. Moreover, to suppress the temperature gradient by the generation of reaction heat in the MH alloy bed, a reactor internal surface area is widely designed as much as possible. In order to act as the heat sink, the thermal capacity of the reactor to the MH alloy is designed by 1000 times or more. Figure 2 shows the details of reactor.

2.2 Experimental procedure and conditions

2.2.1 Experimental methods

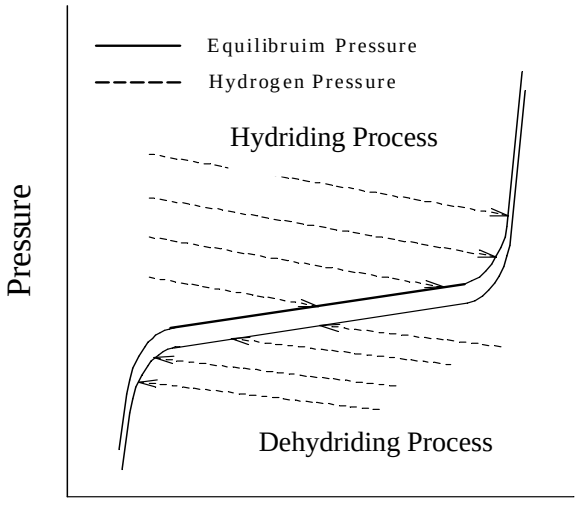

Fig.3 Experimental Procedure

The inner condition of a reactor and reservoir in the reaction rate experiment can be shown by the PCT curve of Fig. 3. It expresses the changing of temperature, hydrogen concentration and pressure of the reactor and the reservoir during the reaction rate experiment. The system pressure change during experiment is expressed by dotted lines. Procedures of hydriding reaction rate experiment are as follows: 1) Close the valve between reactor and reservoir. 2) Supply hydrogen gas of certain pressure to reservoir. 3) Vacuum the reactor which has the activated metal hydride inside, and immerse it into the thermal constant bath. 4) Open the valve between reactor and reservoir. 5) Measure and record the pressure change of the system. 6) Calculate the reaction rate.

For the dehydriding experiment, almost all the procedures are the same as the hydriding test which has listed above. Only hydrogen gas will be supplied to the reactor and the reservoir will be vacuumed every time.

2.2.2 Experimental conditions

Tables 1 and 2 show the pressure and the temperature dependency of the hydriding reaction rate experiment condition. Reservoir capacity in the hydriding reaction rate experiment is 132.2 cm^3 .

Table 1 Hydriding Experimental Conditions of Dependency on Pressure Difference

Temperature	℃	30
Initial Hydrogen Concentration	wt%	0
Pressure Difference	MPa	0.53, 0.64, 0.72, 0.82, 0.91

Table 2 Hydriding Experimental Conditions of Dependency on Temperature

Pressure Difference	MPa	0.63
Initial Hydrogen Concentration	wt%	0
Temperature	℃	30, 50, 70, 90

Moreover, experimental conditions of dehydriding reaction rate are shown in Tables 3 and 4. But, the initial hydrogen concentration of MH in the dehydriding condition cannot be controlled. The condition concerning the dependency of an initial hydrogen concentration of MH is included in these conditions. Reservoir capacity in the dehydriding reaction rate experiment is 80.7 cm^3 .

Table 3 Dehydriding Experimental Conditions of Dependency on Pressure Difference

Temperature	℃	160
Initial Hydrogen Concentration	wt%	about 0.834 (1.5 MPa)
Pressure Difference	MPa	0.41, 0.50, 0.59, 0.68, 0.78

Table 4 Dehydriding Experimental Conditions of Dependency on Temperature and Initial Hydrogen Concentration

Pressure difference, MPa	0.39	
Initial hydrogen concentration, wt%	130℃	0.27, 0.35, 0.43, 0.58
	140℃	0.30, 0.36, 0.41, 0.46
	150℃	0.31, 0.34, 0.40, 0.46
	160℃	0.38, 0.40, 0.46, 0.50

Moreover, MH alloy bed thickness is about 0.9mm in the experiment.

3. Experimental results

3.1 The radius and the packing density of MH particles

The surface area radius r_s and the volume radius r_v of MH particles after the activation are measured by using the scanning electron microscope (SEM). To determine the surface reaction rate Eq. (4) and the diffusion rate Eq. (5), these measured r_s and r_v are substituted, respectively. In addition, the r_s and r_v before activation are also measured. They are shown in the Table 5. As for MH particles size, it is understood that it is atomized down to about 1/40 by the activation.

Table 5 Mean Radius of MH before and after Activation

	Before Activation	After Activation
Surface Radius r_s	0.215 mm	0.00437 mm
Volume Radius r_v	0.219 mm	0.00530 mm

The packing density is estimated using the following assumptions. 1) MH particle is a globular form. 2) The Peret diameter is used as a particle diameter. As a result, this value is 3.665 kg/m^3 .

3.2 The reaction rate of hydriding process

3.2.1 The pressure difference dependency

The reacted fraction *F* at constant temperature (303K), as a function of time *t*, is shown in Fig. 4. Fig.5 shows the relations between *dF/dt* and the reacted fraction *F*. A relatively rapid reaction rate takes place for values of the reacted fraction *F* up to about 0.3. It is evident that hydrogen diffusion plays a minor role during this stage, as that part of the alloy not covered by hydride is always in contact with hydrogen. The surface reaction is therefore postulated as the rate-controlling step. After the alloy particles have been completely covered by a hydride layer, the transport of materials through the layer by diffusion becomes rate-controlling step. At this stage, the reaction rate decreases and becomes slow.

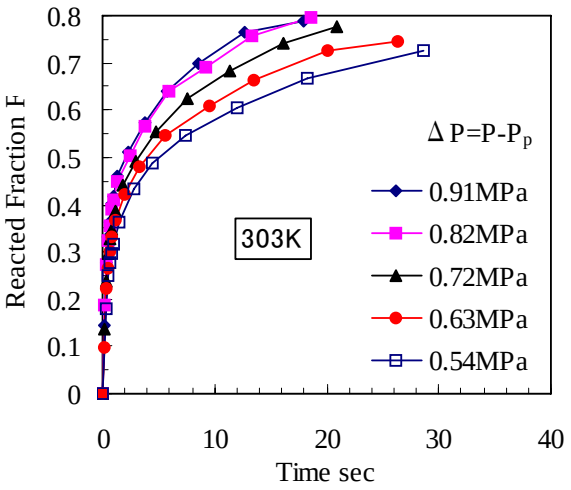

Fig. 4 Hydriding reacted fraction vs. time

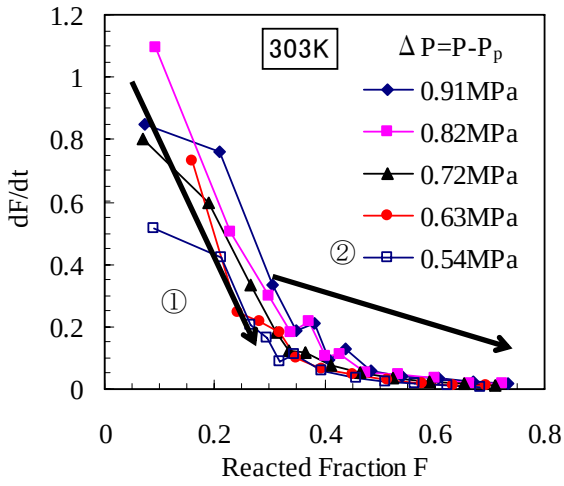

Fig. 5 Hydriding rate-controlling step

After various trials, we attained the result that k_h, k'_h of MH_{High} are governed by the following expressions [4, 5].

$$k_h = k_s g(P, P_p) h(T) / R\rho r_s \quad (2)$$

$$k'_h = 6 D i_h g'(P, P_p) h'(T) / R\rho r_v^2 \quad (3)$$

where k_s is a rate constant in cm/s, Di_h is a diffusion coefficient in cm^2/s. Plots of $1-(1-F)^{1/3}$ and $1-3(1-F')^{2/3}+2(1-F')$ at constant temperature (303K), as a function of time, are shown in Fig.6. k'_h is given by the slope of the straight lines shown in Fig. 6. As ΔP becomes larger, it is recognized that k_h and k'_h are enhanced. The experimental data are possible to be correlated by using the following exponential approximation [6, 7] as function of ΔP among the present approximations.

Surface reaction;

$$k_h = 0.2662\left(P - P_p\right)^{0.58} \tag{4}$$

Diffusion reaction;

$$k'_h = 0.01818\left(P - P_p\right)^{1.62} \tag{5}$$

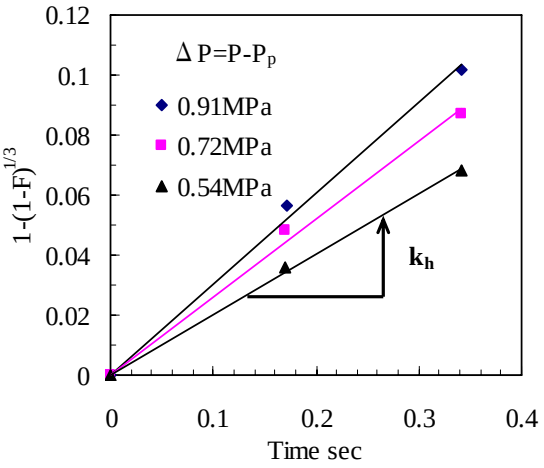

(a) Surface reaction

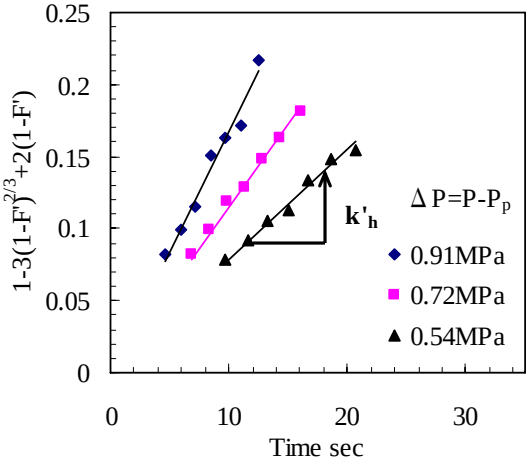

(b) Diffusion reaction

Fig. 6 f(F) as a function of time at 303 K

3.2.2 The temperature dependency

Fig. 7 shows the plots of $1-(1-F)^{1/3}$ and $1-3(1-F')^{2/3}+2(1-F')$ as a function of time at constant ΔP. k_h and k'_h are given by the slope of the straight lines shown in Fig. 7. k_h and k'_h become higher with increasing temperature. After various trials, the temperature dependency of k_h and k'_h can be represented by the Arrhenius expressions [8, 9] and the activation energies are also obtained as shown in Eqs. (6) and (7).

Surface reaction;

$$k_h = 0.2605\exp(-545.7/RT),$$
$$E_{h,s} = 545.7 \ \text{J/mol H}_2 \tag{6}$$

Diffusion reaction;

$$k'_h = 0.7000\exp(-1.214\times10^4/RT),$$
$$E_{h,di} = 1.214\times10^4 \ \text{J/molH}_2 \tag{7}$$

The constant, $k_s = 1.653\times10^{-2}$ and the coefficient, $Di_h = 1.425\times10^{-6}$ in the Eqs. (2) and (3) are estimated by using the above results. Therefore, the brand new rate correlations of hydriding process are expressed as follows.

Surface reaction step $(F < 0.3)$

$$1-(1-F)^{1/3} = k_h t$$
$$k_h = (1.653\times10^{-2}/R\rho r_S) \times\left(P-P_P\right)^{0.58}\times\exp(-545.7/RT) \tag{8}$$

Diffusion reaction step $(F > 0.3)$

$$1-3(1-F')^{2/3}+2\left(1-F'\right) = k'_h t$$
$$k'_h = (6\times1.425\times10^{-6}/R\rho r_V^{\,2}) \times\left(P-P_P\right)^{1.62}\times\exp(-1.214\times10^4/RT) \tag{9}$$

where $F' = (F-F_0)/(1-F_0)$, $F_0 = 0.3$ and F_0 is a reacted fraction at the beginning of diffusion reaction.

3.3 The reaction rate of dehydriding process

3.3.1 The pressure difference dependency

The reacted fraction F at constant temperature (433 K), as a function of time t, is shown in Fig. 8.

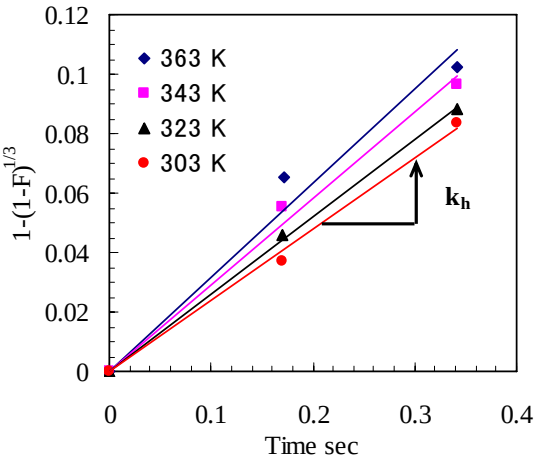

(a) Surface reaction

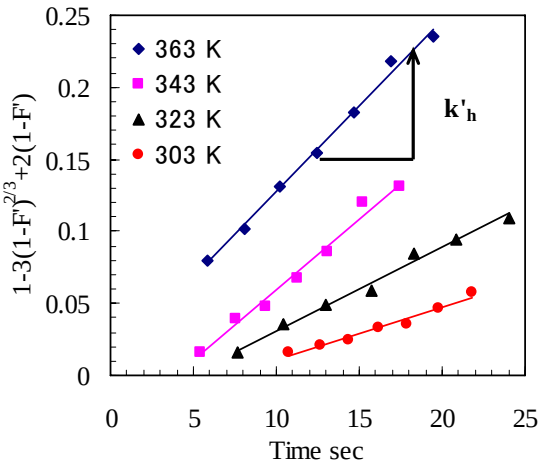

(b) Diffusion reaction

Fig. 7 f(F) as function of time at ΔP =0.63 MPa

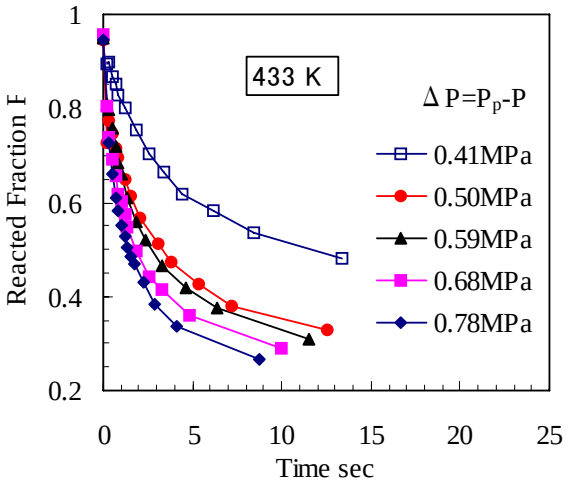

Fig. 8 Dehydriding reacted fraction vs. time

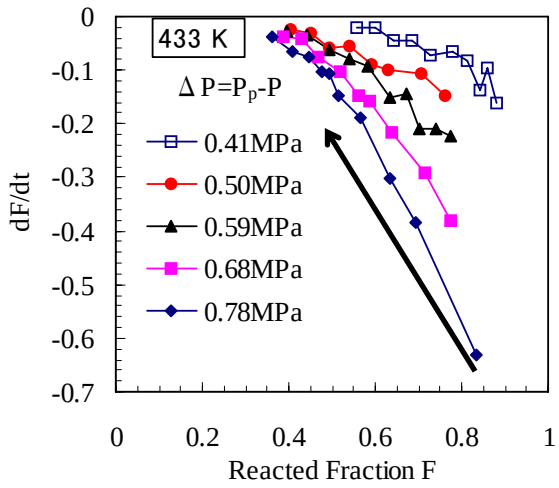

Fig. 9 Dehydriding rate-controlling step

Figure 9 shows the relations between the reaction rate *dF/dt* and the reacted fraction *F*, and it is found out that the dehydriding process is dominated by a unique rate-controlling step.

About the dehydriding process the relations of the reacted fraction *F* vs. time *t* are expressed with the Eq. (9). But, the *F'* of Eq. (9) is calculated as $F'=F_1-F$. F_1 indicates an initial reacted fraction during the dehydriding process. The initial condition of dehydriding experiments coincide with the end of hydride process so that it is difficult to keep the initial reacted fraction F_1 at every test, this effect should be taken into account to the dehydriding process. Therefore, as for the dehydriding process, we propose Eq. (10) by introducing the c_1^{nc} term with respect to F_1.

$$k'_d = (6Di_d / R\rho r_v^2) g'(P_p, P) h'(T) c_1^{nc} \qquad (10)$$

where c_1 is the initial concentration of the dehydriding process in wt %.

Plots of $1-3(1-F')^{2/3}+2(1-F')$ at constant temperature (433K), as a function of time, are shown in Fig.10. The reaction rates k'_d are given by the slopes of the straight lines shown in Fig.10. The qualitative trend of k'_d to ΔP is almost similar as those of k_s and k'_s. The correlate of experimental data is also possible by the exponential function [6, 7] of the pressure difference ΔP such as Eq. (11).

$$k'_d = 0.085(P_p - P)^{1.8} \qquad (11)$$

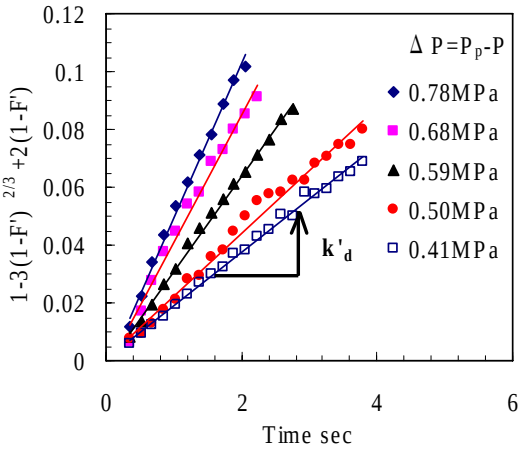

Fig. 10 f (F) as function of time at 433K

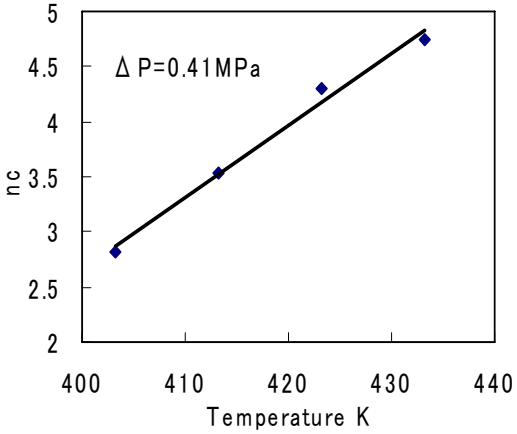

Fig. 12 nc vs. temperature

3.3.2 The temperature and the initial reacted fraction dependency

A plot of the reaction rate k'_d at the constant temperature (403K), and the constant ΔP (0.41MPa), with respect to c_1, is shown in Fig.11.

The tendency of these experimental data can be related to the exponential function of the c_1 as shown Eq. (12). And, the relation of the nc vs. the temperature at constant ΔP (0.41 MPa) is illustrated in Fig.12.

$$k'_d \propto c_1^{nc} = 0.00495 c_1^{2.82} = 0.00495 c_1^{0.066T-23.58} \tag{12}$$

The Arrhenius plot [8, 9] for the apparent rate constant defined as the k'_d / c_l^{nc} at the constant ΔP (0.41 MPa) is shown in Fig. 13. The activation energy of dehydriding process is found to be -7.1×10^4 J/molH_2. From the above, the constant Di_d of the Eq. (10) is decided as 62.07. Therefore, it can get the brand new rate equation of the dehydriding process as follows;

$$1-3(1-F')^{2/3}+2(1-F') = k'_d\, t$$
$$k'_d = (6\times 62.07 / R\rho r_d^2)\times(P_P - P)^{1.8} \times \exp(-7.1\times10^4 / RT)\times c_1^{0.0066T-23.58} \tag{13}$$

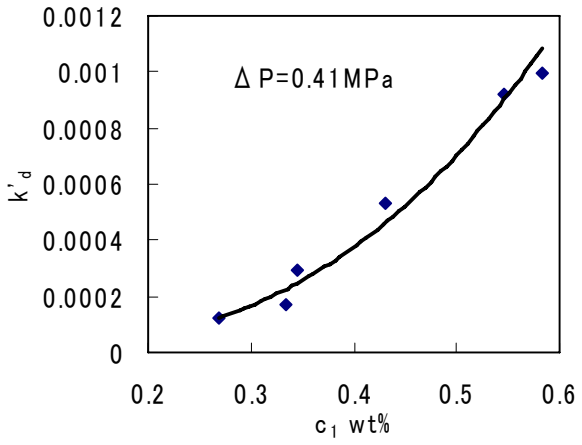

Fig. 11 Dependency of k'_d on initial concentration at 403 K

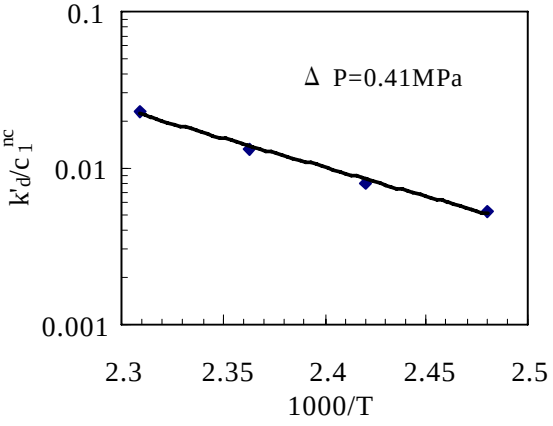

Fig. 13 Arrhenius plot of dehydriding process

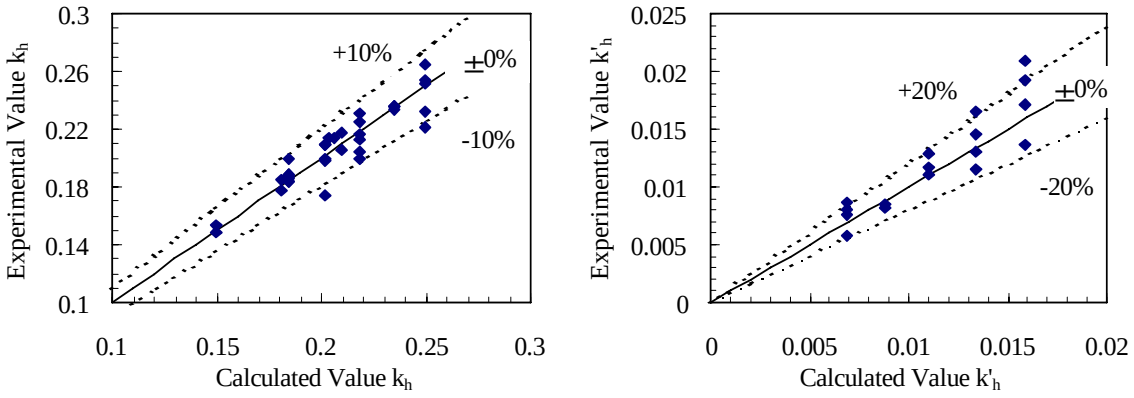

(a) Surface reaction (b) Diffusion reaction

Fig.14 Calculated data vs. experimental data in hydriding process

3.4 Comparison

3.4.1 Hydriding process.

Comparison between experimental reaction rates and predictions is made and represents in Fig.14. As for the surface reaction step, the experimental results are expressed by the brand new rate Eq. (8) in the error within ±10%. Additionally, as for diffusion reaction step, the experimental data agrees with prediction using brand new rate correlation within ±20 %.

3.4.2 Dehydriding process

On the other hand, for the dehydriding process, it is understood that the experimental data are predicted by the brand new rate Eq. (13) in the error within ±15% from the comparison.

4. Conclusion

In the initial stage of the hydriding process of MH_{High} ($F<0.3$) the rate-controlling step is a surface reaction. And, at a later stage of the hydriding process ($F>0.3$) the diffusion reaction is the rate controlling step. As for the dehydriding process, it is understood that only diffusion reaction is the rate-controlling step. The reaction rates are exponentially proportional to the pressure difference and increases with temperature. The experimental reaction rates of MH_{High} are represented by the brand new rate correlations in the error within ±20 %. As shown in our experimental results, because the reaction of MH_{High} becomes a saturated condition within 20 seconds, it can be used for the heat driven type MH refrigerator.

Acknowledgements

This work has been partially funded by Waseda Advanced Research Institute of Science and Engineering.

References

[1] Takeda, H. , Kabutomori, T., Murai, M. and Jin, T., JSW technical report, No.54, (1998), 39-46.
[2] Uehara, I., Sakai, T. and Ishikawa, H., Journal of Alloys and Compounds, Vol. 253-254, (1997), 635-641.
[3] Rudman, P. S., Journal of the Less-Common Metals, Vol. 89, (1983), 93-110.
[4] Stander, C. M., Physic. Chemie Neue Folge, (1977), 229-238.
[5] Levenspiel O., Chemical Reaction Engineering, John Wiley & Sons, Inc., (1972).
[6] Suda, S. and Komazaki, Y., Journal of the Less-Common Metals, Vol. 89, (1983), 127-132.
[7] Suda, S., Kobayashi, N. and Yoshida, K., *ibid.*, Vol. 73, (1980), 119-126.
[8] Wang, X. L. and Suda, S., *ibid.*, Vol. 159, (1990), 83-90.
[9] Han, S. C. and Lee, J. Y., *ibid.*, Vol. 128, (1987), 155-165.